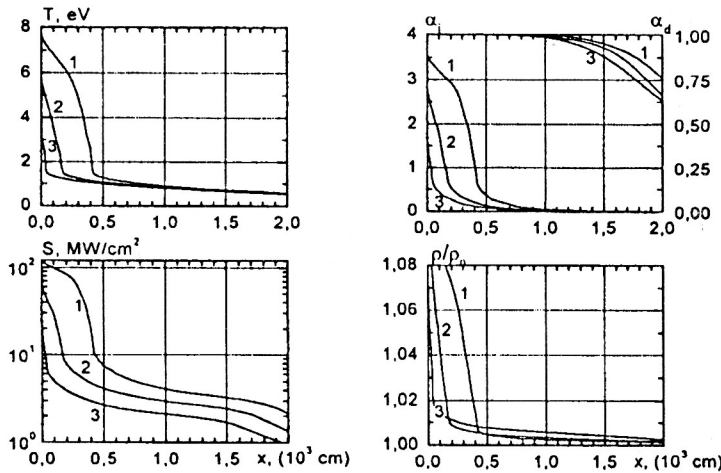


POWERFUL SHOCK WAVES RADIATION IN AIR II

K.L. STEPANOV, L.K. STANCHITS, Y.A. STANKEVICH

Heat & Mass Transfer Institute, ul. Brovky, 15, 220072, Minsk, Belarus
E-mail kls@hmti.ac.by

5. Calculation results. Further we shall consider the spatial structure of shock waves. Fig.7 illustrates the results of calculations of physical characteristics in the warming up zone before the shock wave at altitudes 30 km (in this case for convenience the wave is moving from left to right). The dependence on distance from the front of temperature, radiation flux, degrees of dissociation and ionization of air and compression in shock waves being propagated at velocities $D = 50, 40$ and 30 km/s is shown. Waves with such D at $H > 30$ km are supercritical ones. Comparison of the dependence of a radiation flux and parameters α_p, α_i shows that maximum flow divergences correspond to



sections where intensive gas disassociation and ionization takes place. As seen from the plots, disassociation and ionization waves are sufficiently strongly separated in space.

Fig. 7. Spatial parameter profiles at altitude $H=30$ km.
1 - $D=50$ km/s,
2 - $D=40$ km/s,
3 - $D=30$ km/s.

First of all it is necessary to note the very strong dependence of warming up area spatial scales on altitude. In particular, the ratio of distances from the front, at which temperature $T=1$ eV, at appropriate velocities is equal $(X_{50}/X_{40})_{T=1} \approx 40$ and $(X_{50}/X_{30})_{T=1} \approx 1.6 \cdot 10^3$ for all $D > 30$ km/s. The ratio of distances, where the air completely is dissociated, $(X_{50}/X_{40})_{\alpha_d=1} \approx 35$ and $(X_{50}/X_{30})_{\alpha_d=1} \approx 1.5 \cdot 10^3$ and also poorly depends on the SW velocity. The ratio of distances from the front, on which single ionization of gas ($\alpha_i=1$) is achieved, is equal $(X_{50}/X_{40})_{\alpha_i=1} = 40 - 50$ and $(X_{50}/X_{30})_{\alpha_i=1} = (2 - 5) \cdot 10^3$. At alteration of the altitude from $H=40$ to $H=50$ km the air density is reduced by a factor of 4, and the ratio of densities at altitudes 30 and 50 km is $\rho_{30}/\rho_{50} = 18$. If it is taken into account that in the range of temperatures $T = 1-10$ eV the average Rosseland path of radiation is well approximated by dependence $L_R \sim \rho_0^{-\beta}$ where $\beta \approx 1.5$, it appears that it increases $(L_{50}/L_{40})_R = 8$ and $(L_{50}/L_{30})_R = 76$ times.

Therefore, the ratio of warming up area scales at various altitudes is approximately $(X_{H_1} / X_{H_2})_{T=1} = [(L_R / \rho_0)_{H_1} / (L_R / \rho_0)_{H_2}]$. Estimated data on the mass of the air layer heated by radiation (the area with $T \geq 1$ eV) for the considered modes of SW propagation are presented in Table 2 ($M \approx \rho_0 X_{T=1}$).

Table 1. Mass of gas heated by shock wave radiation (g/cm²)

	D=50 km/s	D=40 km/s	D=30 km/s
H=50 km	1.5+0	1.0+0	7.0-1
H=40 km	1.5-1	1.0-1	7.0-2
H=30 km	1.5-2	1.0-2	7.0-3

The structure of SWs at altitude H=20 km with D=20 and D=50 km/s is presented in fig.8. In distinction from the previous data, the parameter profiles are given here for the area behind the SW front too. The following parameters are presented: temperature, radiation flux S and radiation flux in the "visible" area of the spectrum S_{vis} ($1.5 < E < 6.5$ eV, up to band Schumann-Runge), degrees of ionization and dissociation, free length in the visible range averaged on the local spectrum of radiation l_{vis} .

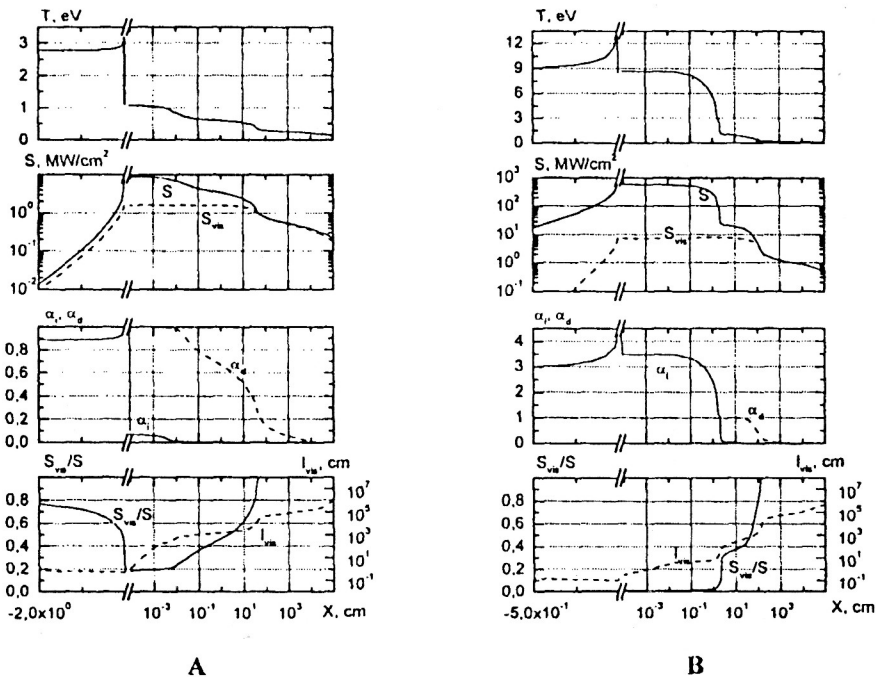


Fig. 8. Shock wave structure at H=20 km. A - D=20 km/s, B - D=50 km/s.

It is seen that at D=20 km/s "visible" radiation contain at SWF near 15% of full flux, at distance from front 40 cm radiative flux is completely "visible". For wave with D=50 km/s this part contain not much larger 1% at SWF and is completely "visible" at 10² cm from it. It is interesting nonmonotone alteration of the degree of ionization α₁. For ex-

ample, for $H=20$ km and $D=50$ km/s in precursor zone near SWF $\alpha_1=3.5$, behind front is 4.2 and in final state $\alpha_1=3$.

The spectra of radiation of shock waves at various distances from the viscous jump are presented on fig.9 and 10 for series D and H. The spectra of black-body radiation with equilibrium temperature T_1 and peak temperature T_2 are specified on the wave front. It is seen that for quantum with $E \leq 7$ eV the temperature peak is optically transparent, the radiation in this area is close to Planck radiation with T_1 . The radiation flux in spectral lines is closer to $B_E(T_2)$. As a whole, the temperature peak radiates a spectrum characteristic for semitransparent layer.

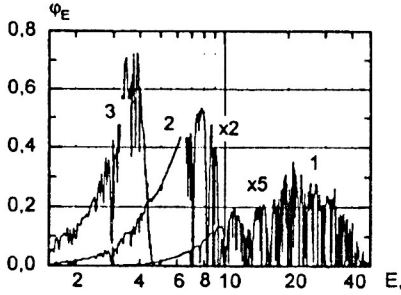


Fig. 9. Normalized spectrum of SW with $D=50$ km/s at $H=30$ km. 1 - distance from SWF $x=50$ cm $S=107$ MW/cm²; 2 - $x=10^3$, $S=4$; 3 - $x=10^4$, $S=0.27$.

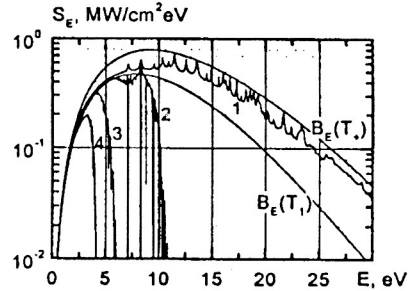


Fig. 10. Spectral radiation flux of SW with $D=20$ km/s at $H=20$ km. 1 - $x=0$, $S=8.76$ MW/cm²; 2 - $x=4$ cm, $S=2.92$; 3 - $x=55$, $S=0.93$; 4 - $x=9.2 \cdot 10^3$, $S=0.405$.

The space distributions of spectral and integrated radiation fluxes are determined by opacity of the air. At adequately large distances the entire radiation is concentrated in the visible area of the spectrum. The absorption coefficient in this range is small in comparison with other spectrum sections where the SW radiates. At temperatures $\sim 10^3$ K the absorption coefficient (Avilova, 1970; Landshoff, 1969) poorly depends on T , its dependence on quantum energy and density can be approximated by expression $\lg \kappa_E = E(4.33 - 0.66E) - 11.4 + 1.5 \lg(\rho/\rho_0)$, where quantum energy E in eV and $\rho_0 = 1.23 \cdot 10^{-3}$ g/cm³. The free length (with $E=3$ eV) in "cold" air at $H=30$ km is $\sim 10^7$ cm.

At analysis of radiation exiting to "infinity" it is conventionally assumed that cold air is transparent for visible light. Noticeable absorption begins in the Schumann-Runge band at wave lengths $\lambda \leq 190$ nm. Large though final free lengths of visible radiation cause heating of gas up to temperatures $T \sim (1-3) \cdot 10^3$ K at large distances, the radiation flux is exponentially reduced. Therefore, the largest physical scale, which is the distance from the SW front to the boundary of the air dissociation area, can be adopted as the width of the warming zone. The radiation exiting from this boundary (conditionally $\alpha_4 \approx 0.05$) is in the visible spectrum band and weakly excites the initial medium parameters. It may be considered as exiting to "infinity". When noticeable dissociation of air before the front is absent, the radiation exiting from the SW front practically is not screened. In this case the shock wave radiates as a black body with equilibrium tempera-

ture T_1 , and the radiation flux to "infinity" is equal to the fraction of the visible spectrum of the total radiative flux σT_1^4 . The flux of radiation exiting to "infinity" S_∞ and its fraction relative to the hydrodynamic flow of energy S_G thus calculated are contained in table 2. The results for S_∞ and α indicated in the usual font, were obtained according to

Table 2. SW energy flow $S_G = \rho_0 D^3 / 2$ (MW/cm²), flux S_∞ and ratio $\alpha = S_\infty / S_G$ (%)

H		D				
		50	40	30	20	10
50	S_G	6.375	3.264	1.377	4.08-1	5.1-2
	S_∞	1.2-2	9.7-3	7.2-3	4.8-3	2.5-3
	α	1.88-1	2.97-1	5.23-1	1.18	4.9
40	S_G	2.54+1	1.30+1	5.495	1.628	2.035-1
	S_∞	5.2-2	4.1-2	3.1-2	2.07-2	1.04-2
	α	2.05-1	3.4-1	6.16-1	1.39	5.1
30	S_G	1.15+2	5.888+1	2.484+1	7.360	9.20-1
	S_∞	2.55-1	2.03-1	1.53-1	1.02-1	4.7-2
	α	2.22-1	3.45-1	6.2-1	1.4	5.1
20	S_G	5.556+2	2.845+2	1.200+2	3.556+1	4.445
	S_∞	1.32	1.08	8.08-1	5.37-1	1.0-1
	α	2.37-1	3.8-1	6.73-1	1.51	2.81
10	S_G	2.619+3	1.341+3	5.657+2	1.676+2	2.095+1
	S_∞	6.96	5.57	4.19	2.8	1.28-1
	α	2.66-1	4.15-1	7.4-1	1.67	6.9-1
0	S_G	7.688+3	3.936+3	1.660+3	4.920+2	6.15+1
	S_∞	2.21+1	17.7	12.9	8.61	1.65-1
	α	2.88-1	4.5-1	7.77-1	1.75	2.68-1

criterion $\alpha_d \approx 0.05$. For weaker shock waves ($D=10$ km/s, $H=20$ and 10 km) the gas before the front is not dissociated, and $S_\infty = \beta_{\text{vis}} \sigma T_1^4$ (bold font).

References

- Romanov G.S., Stankevich Yu.A., Stanchits L.K. and Stepanov K.L.: 1995 Int. J. Heat Mass Transfer, **38**, 545.
 Romanov G.S., Stepanov K.L. and Stanchits L.K.: 1988 Sov. Plasma Physics, **14**, 1383.
 Panasenko L.N., Romanov G.S., Stankevich Yu.A. and Stepanov K.L.: 1995 Russian Engineer-Physical J, **68**, 569.
 Stepanov K.L., Stanchits L.K., Stankevich Yu.A.: 1998, Preprint of Heat & Mass Transfer Institute №2, Minsk.
 Zeldovich Ya.B., Raiser Yu.P. Physics of Shock Waves and High Temperature Hydrodynamic Phenomena. Moscow, Nauka, 1966.
 Avilova I.V., Biberman L.M., Vorob'ev V.S. et al. The Optical Properties of Hot Air. Moscow, Nauka, 1970.
 Landshoff R.K.M., Magee J.L. Thermal Radiation Phenomena. V.I. Radiative Properties of Air. N.Y.-W. 1969.